Molecular fragments in the Carina Flare supershell

R. Wünsch J. Palouš J. E. Dale A. P. Whitworth
S. Ehlerová P. Jáchym V. Sidorin F. Dinnbier
R. Smith J. Dawson Y. Fukui

15th April 2014 / 7 years in Chile workshop

Introduction

- Subject of this work: secondary star formation triggered by expanding shells (collect and collapse model)
- Aim: compare theoretical models of fragmentation of the self-gravitating shell with observations of fragmenting (super-)shells

Outline:

1. Hydrodynamic simulations (AMR and SPH) of gravitationally unstable shell and their comparison with each other and with theoretical models.
2. APEX ^{13}CO observations of a part of the Carina Flare supershell (GSH287+04-17) and analysis of fragment properties

Introduction

- Subject of this work: secondary star formation triggered by expanding shells (collect and collapse model)
- Aim: compare theoretical models of fragmentation of the self-gravitating shell with observations of fragmenting (super-)shells

Outline:

1. Hydrodynamic simulations (AMR and SPH) of gravitationally unstable shell and their comparison with each other and with theoretical models.
2. APEX ^{13}CO observations of a part of the Carina Flare supershell (GSH287+04-17) and analysis of fragment properties

Introduction

- Subject of this work: secondary star formation triggered by expanding shells (collect and collapse model)
- Aim: compare theoretical models of fragmentation of the self-gravitating shell with observations of fragmenting (super-)shells

Outline:

1. Hydrodynamic simulations (AMR and SPH) of gravitationally unstable shell and their comparison with each other and with theoretical models.
2. APEX ^{13}CO observations of a part of the Carina Flare supershell (GSH287+04-17) and analysis of fragment properties

Simulation setup

- extremely simplified model to avoid instabilities other than the gravitational one (RT, Vishniac)
- ballistic shell in a rarefied medium with non-zero pressure

$M_{\rm shell} = 2 \times 10^4\ \mathrm{M}_\odot$
$T_{\rm shell} = 10\ \mathrm{K}$
$R_{\rm shell,0} = 10\ \mathrm{pc}$
$V_{\rm shell,0} = 2.2\ \mathrm{km\,s^{-1}}$
$R_{\rm shell,max} = 23\ \mathrm{pc}$
$P_{\rm ext} = 10^{-17}, 10^{-13}$
or $5 \times 10^{-13}\ \mathrm{dyne\,cm^{-2}}$

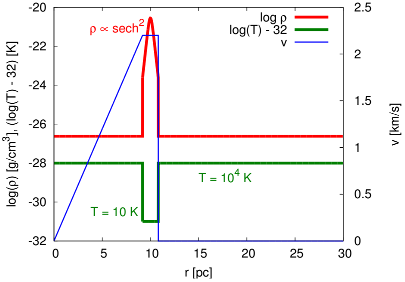

Codes & initial conditions

- AMR: Flash 2.5 (Fryxell et al., 2000), resolution: 640^3
- SPH: SPHNG (Bate, Bonnell & Price, 1995), res.: 1.2×10^6 ptcls
- remapping: noise due to SPH particles remapped on the grid
- random velocities: Gaussian with $\sigma = c_s$

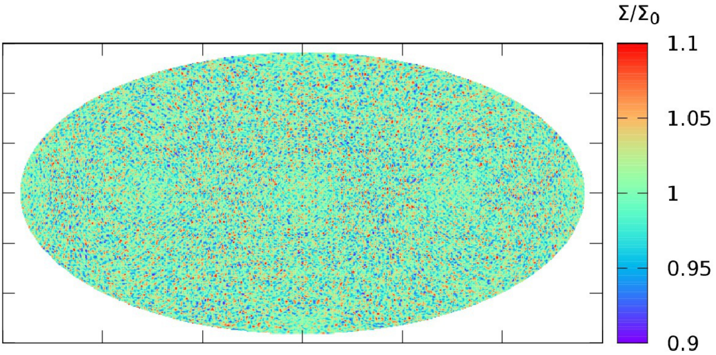

AMR vs. SPH

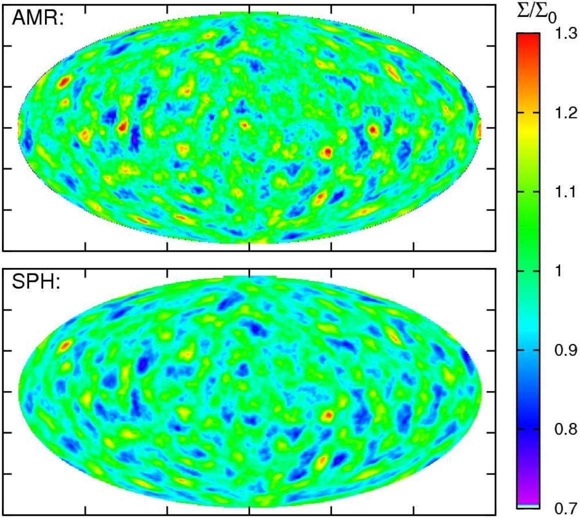

AMR vs. SPH

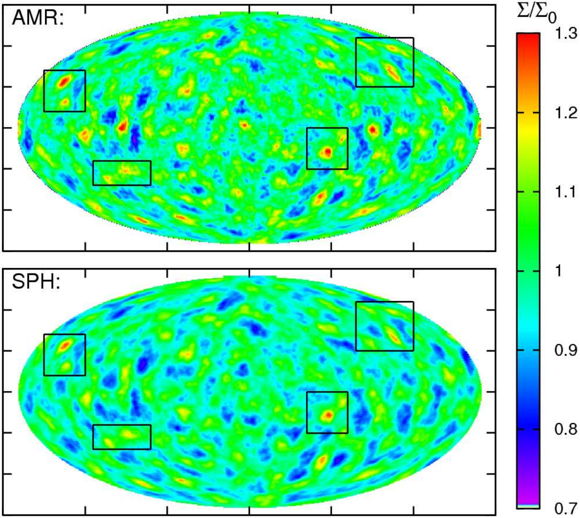

Perturbation growth rate

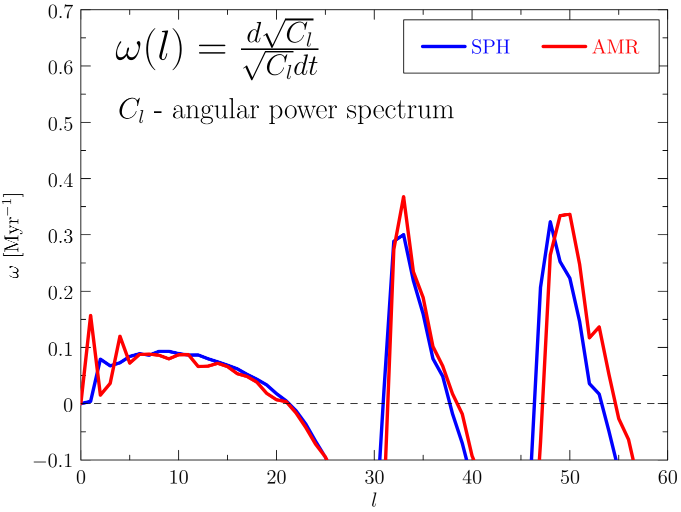

Perturbation growth rate

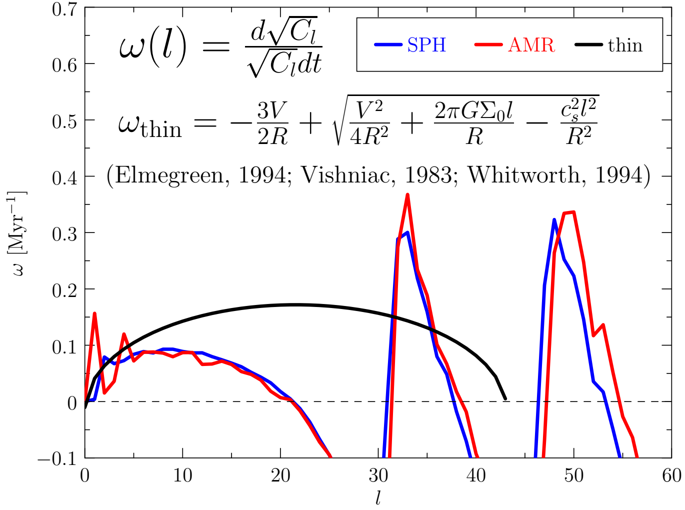

Perturbation growth rate

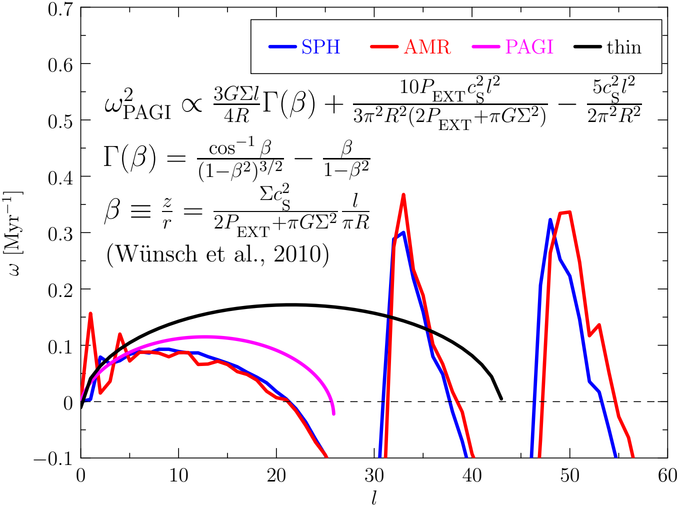

$P_{\rm EXT}$ determines gravitational instability wavelength

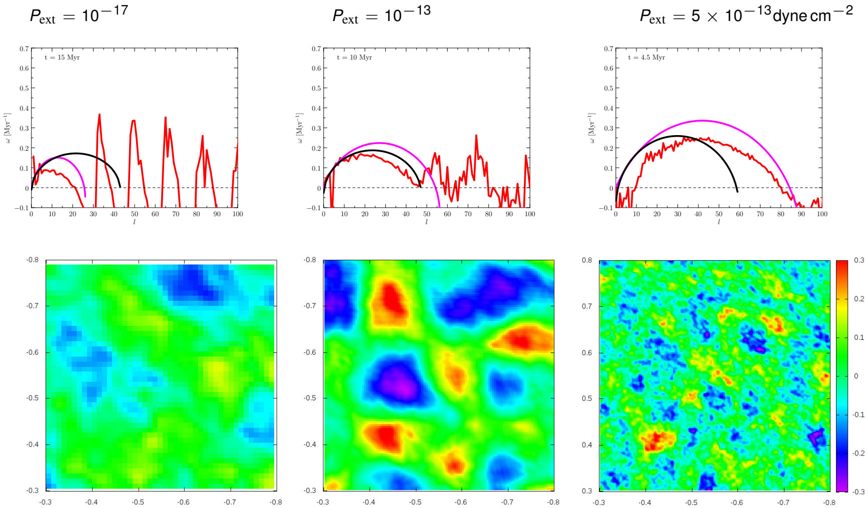

- further improved by Kim et al. (2012) (for high $P_{\rm ext}$)
- high accuracy numerical tests by F. Dinnbier

Carina Flare supershell (discovered by Fukui, 1999)

- we observe a part of the Carina Flare supershell (GS287+4-17) with APEX/SHFI
- CF extends $\sim$ 450 pc above the gal. pl. - different P_{EXT} expected
- two clouds (16 and 74) selected (based on NANTEN obs.)
- Cloud 16: 22 hours (86A), $dv = 0.6$ km/s
- Cloud 74: 36 hours (89A), $dv = 0.1$ km/s

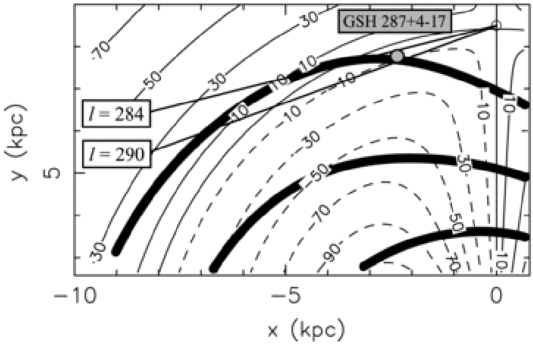

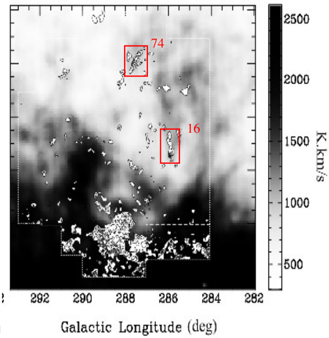

APEX vs. NANTEN

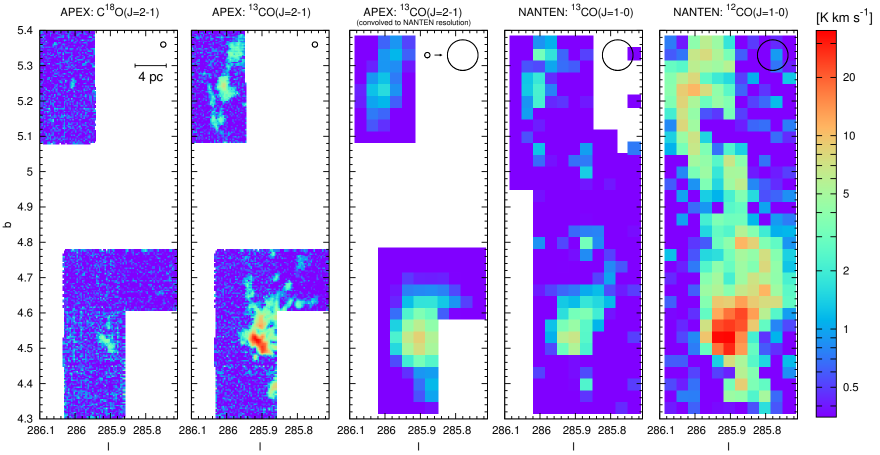

Identification of clumps: cloud 16

- clump-finding code DENDROFIND
  (http://galaxy.asu.cas.cz/∼richard/dendrofind/)
  (Wünsch et al., 2012, A&A, 539, 116)
- two essential parameters: `Tcutoff`, `dTleaf`

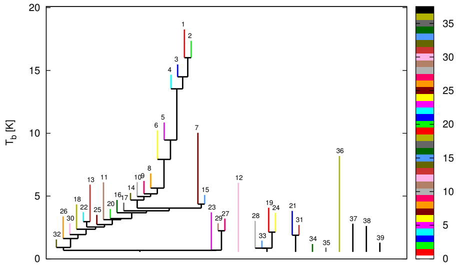

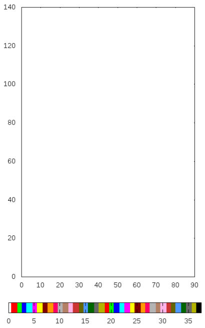

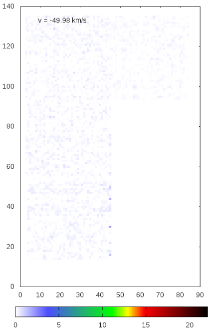

Identification of clumps: cloud 74

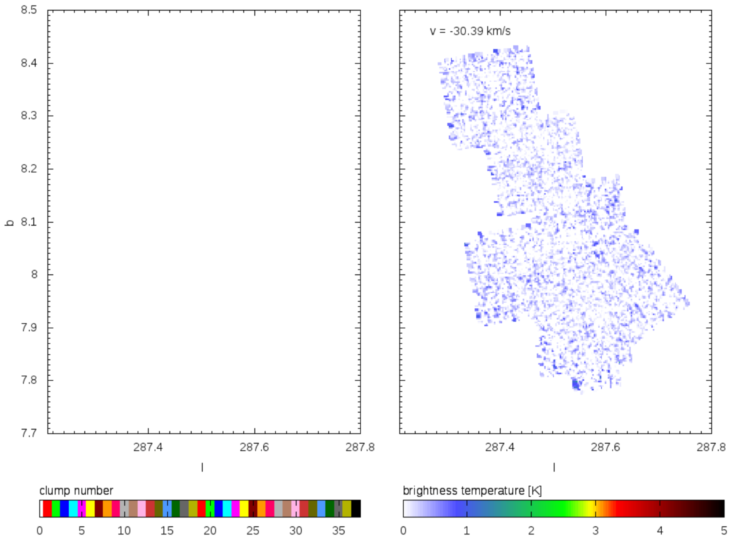

Clump mass spectrum & clump distances

- cloud 16:
  $dv = 0.6$ km/s, 44 clumps, CMF peak: $\sim 10\ M_\odot$
  separation of clumps: minimum spanning tree, $d_{\rm av} \sim 1.7$ pc
- cloud 74:
  $dv = 0.1$ km/s, 235 clumps, CMF break: $\sim 10\ M_\odot$
  separation of clumps: minimum spanning tree, $d_{\rm av} \sim 3.5$ pc

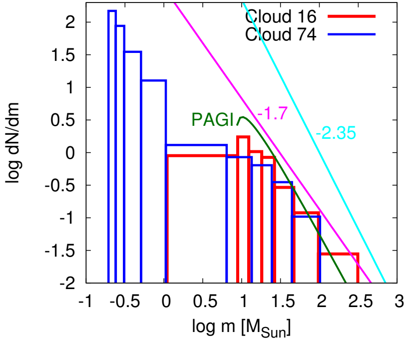

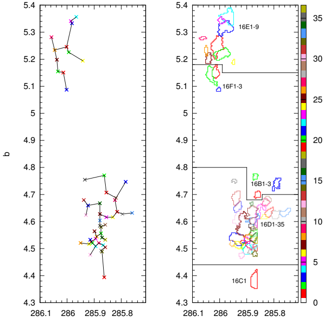

Cumulative CMF

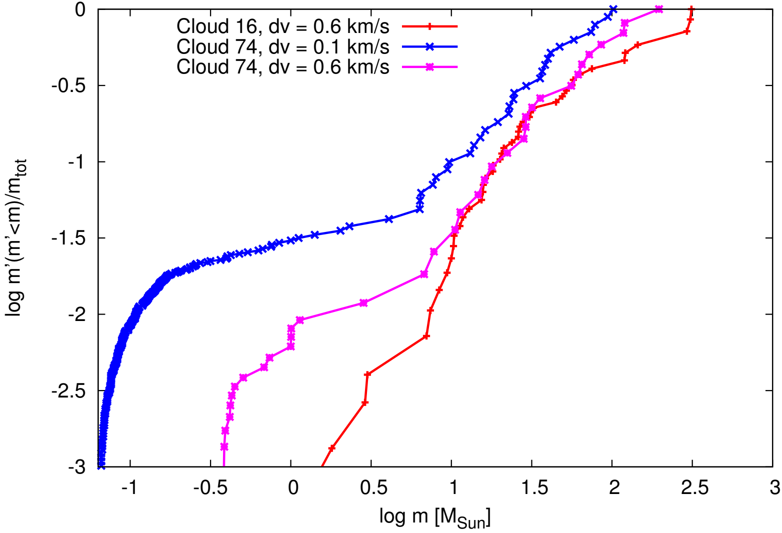

Comparison to PAGI

- contours of constant peak mass of CMF

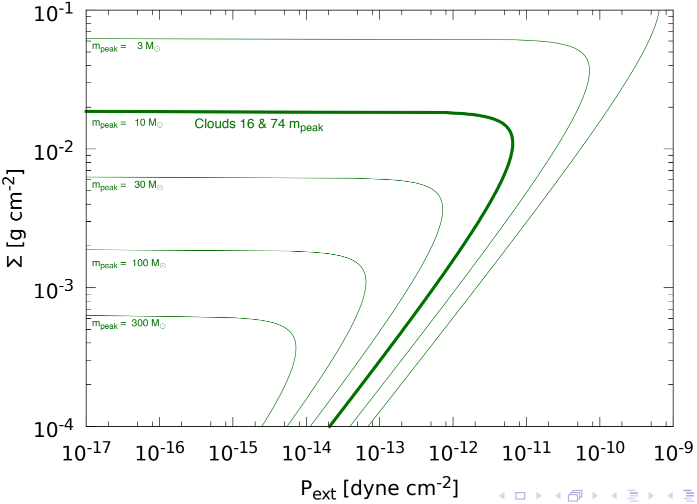

Comparison to PAGI

- contours of constant distance among clumps

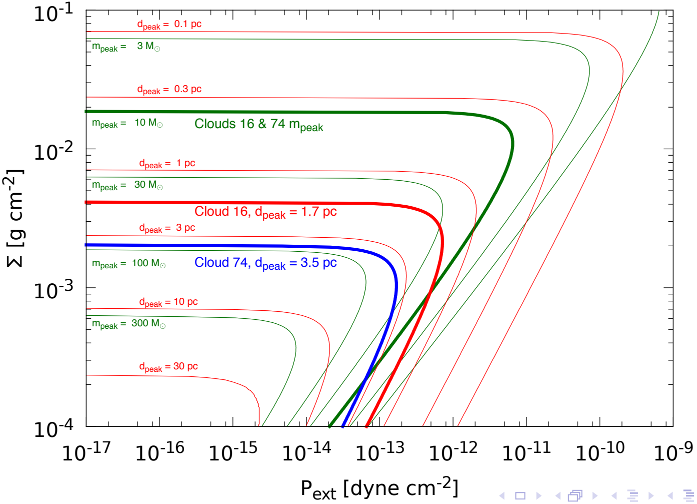

Comparison to PAGI

- average surface density of the Carina Flare supreshell ($\Sigma_{\mathrm{CarinaFlare}}$) and typical pressure in the ISM (P_{ISM})

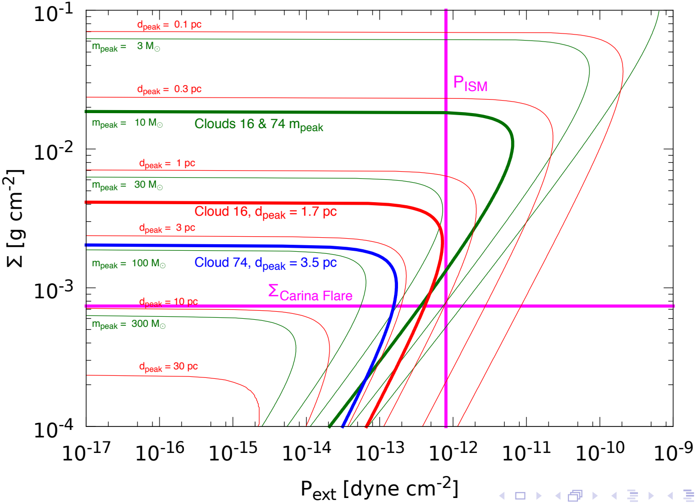

Conclusions

- excellent agreement between AMR and SPH simulations
- results well described by the theory of the thick shell gravitational instability
- cloud 16: CMF and typical distances among clumps consistent with the gravitational instability origin
- cloud 16: the surface density and the external pressure derived from clump properties in agreement with global properties of the CF supershell
- cloud 74: more complex; if clumps formed by gravity, it would suggest lower shell surface density and lower P_{EXT}; however, population of low mass clumps indicates other mechanism must be also involved

Conclusions

- excellent agreement between AMR and SPH simulations
- results well described by the theory of the thick shell gravitational instability
- cloud 16: CMF and typical distances among clumps consistent with the gravitational instability origin
- cloud 16: the surface density and the external pressure derived from clump properties in agreement with global properties of the CF supershell
- cloud 74: more complex; if clumps formed by gravity, it would suggest lower shell surface density and lower P_{EXT}; however, population of low mass clumps indicates other mechanism must be also involved

Conclusions

- excellent agreement between AMR and SPH simulations
- results well described by the theory of the thick shell gravitational instability
- cloud 16: CMF and typical distances among clumps consistent with the gravitational instability origin
- cloud 16: the surface density and the external pressure derived from clump properties in agreement with global properties of the CF supershell
- cloud 74: more complex; if clumps formed by gravity, it would suggest lower shell surface density and lower P_{EXT}; however, population of low mass clumps indicates other mechanism must be also involved

Conclusions

- excellent agreement between AMR and SPH simulations
- results well described by the theory of the thick shell gravitational instability
- cloud 16: CMF and typical distances among clumps consistent with the gravitational instability origin
- cloud 16: the surface density and the external pressure derived from clump properties in agreement with global properties of the CF supershell
- cloud 74: more complex; if clumps formed by gravity, it would suggest lower shell surface density and lower P_{EXT}; however, population of low mass clumps indicates other mechanism must be also involved

Conclusions

- excellent agreement between AMR and SPH simulations
- results well described by the theory of the thick shell gravitational instability
- cloud 16: CMF and typical distances among clumps consistent with the gravitational instability origin
- cloud 16: the surface density and the external pressure derived from clump properties in agreement with global properties of the CF supershell
- cloud 74: more complex; if clumps formed by gravity, it would suggest lower shell surface density and lower $P_{\rm EXT}$; however, population of low mass clumps indicates other mechanism must be also involved